



LAWRENCE  
LIVERMORE  
NATIONAL  
LABORATORY

# Ionic Liquids for Carbon Capture: Solubility Computation Using an Implicit Solvent Model

A. Maiti

January 3, 2013

Applications of Molecular Modeling to Challenges in Clean  
Energy

## **Disclaimer**

---

This document was prepared as an account of work sponsored by an agency of the United States government. Neither the United States government nor Lawrence Livermore National Security, LLC, nor any of their employees makes any warranty, expressed or implied, or assumes any legal liability or responsibility for the accuracy, completeness, or usefulness of any information, apparatus, product, or process disclosed, or represents that its use would not infringe privately owned rights. Reference herein to any specific commercial product, process, or service by trade name, trademark, manufacturer, or otherwise does not necessarily constitute or imply its endorsement, recommendation, or favoring by the United States government or Lawrence Livermore National Security, LLC. The views and opinions of authors expressed herein do not necessarily state or reflect those of the United States government or Lawrence Livermore National Security, LLC, and shall not be used for advertising or product endorsement purposes.

# Ionic Liquids for Carbon Capture – solubility computation using an implicit solvent model

Amitesh Maiti\*

Lawrence Livermore National Laboratory, Livermore, CA 94550, USA

Through a large number of solubility measurements over the last decade and a half, Ionic Liquids (ILs) have been demonstrated as a great medium for the physical dissolution of CO<sub>2</sub>. However, there are numerous possible variations on the component ions of an IL, only a small fraction of which has actually been synthesized so far. In order to screen for the best solvents it is necessary to adopt a theoretical approach that can quickly compute the CO<sub>2</sub> solubility with reasonable quantitative accuracy. Here we report a theoretical prescription that involves computing the chemical potential of CO<sub>2</sub> in the solvent phase with a density-functional-theory-based implicit solvation code (COSMO-RS) and computing the gas fugacity with a cubic equation of state. The approach yields excellent agreement with a large volume of experimental data on CO<sub>2</sub> solubility in diverse classes of ILs over a wide range of temperatures and pressures. The resulting quantitative trends can be used to discover solvents with much higher CO<sub>2</sub> uptake per kg of solvent than has been experimentally achieved so far.

## Introduction

With the status of CO<sub>2</sub> as a prominent greenhouse gas and a major contributor to the global climate change now established, major efforts are being put forth by governments and private agencies in order to cut down CO<sub>2</sub> emission into the atmosphere. Research efforts are focusing on developing technologies in the areas of CO<sub>2</sub> capture, storage, monitoring, mitigation, and verification [1]. The very first step, *i.e.*, capture, is the separation of CO<sub>2</sub> from emissions sources, *e.g.*, flue gas in a coal-fired power plant, and the recovery of a concentrated stream of CO<sub>2</sub> that is amenable to sequestration or conversion. Given that CO<sub>2</sub> in the flue gas is present only in dilute quantities, ~ 10-14% by volume, the common strategy of carbon capture has so far involved chemical absorption in amine-based solvents [2]. Much of the effort has so far involved aqueous solutions of monoethanolamine (MEA). Pilot plants have implemented MEA-based capture systems, although at a scale that is an order-of-magnitude smaller than that required for commercial power plants. Unfortunately, MEA has some shortcomings including, somewhat nonselective against other pollutants, prone to degradation and equipment corrosion, unstable at high concentrations, and finite vapor pressure that results in solvent loss and environmental pollution. Besides, a chemical absorption based strategy is typically associated with a large energy cost in solvent regeneration.

With the above deficiencies in mind, there has been a significant effort in exploring and designing solvents that adsorb CO<sub>2</sub> molecules, *i.e.*, physically bind them without involving any chemical reactions. Ionic Liquids (ILs) [3, 4] constitute such an alternative solvent system that offer distinct advantages over traditional solvents like MEA, some of which include: (1) high chemical stability; (2) low corrosion; (3) almost zero vapor pressure; (4) supportable on membranes [5]; and (5) a huge library of anion and cation choices, which can be potentially optimized for CO<sub>2</sub> solubility and selectivity.

---

\* E-mail: amaiti@llnl.gov

Over the last few years several ILs have been experimentally demonstrated [6-13] to be efficient solvents for CO<sub>2</sub>. A collection of this data does provide useful trends that can be used to optimize the choice of ILs for CO<sub>2</sub> capture. However, each new experiment costs time and money, and is often hindered by the fact that a specific IL may not be readily available. To this end, it is highly desirable to have a computational/theoretical tool that can quickly and accurately compute CO<sub>2</sub> solubility in any solvent (as a function of pressure and temperature). Atomic level simulations, molecular dynamics, Monte Carlo, or binding-energy calculations can provide useful insights into the interactions of CO<sub>2</sub> with the cation and the anion [14-16]. However, predicting solubility involves determining the difference in chemical potential between the solute in the solvent phase and the solute in its source phase. There are theoretical procedures to compute such chemical potential differences from first-principles, e.g., through simulations using advanced sampling techniques, e.g., umbrella sampling [17], free energy perturbation [18], thermodynamic integration [19], or constrained molecular dynamics [20]. However, a successful use of such techniques in complex molecular systems like ILs has its challenges, including large ion sizes, high viscosity, low mobility, and often the lack of interaction parameters.

### Computational Strategy

For fast computation of solubility in a wide variety of solvents it is thus desirable to adopt a quantum-chemistry-based strategy with a large coverage of the periodic table. At the same time, it should be able to yield quantities averaged over orientational and configurational degrees of freedom of the solvent molecules. A widely used method in this regard is the implicit solvent method called COSMO-RS (COnductor-like Screening Model for Real Solvents) [21, 22], in which one represents both the solute and the solvent molecules by the histogram of their surface screening charges called the  $\sigma$ -profile. All interactions, including coulombic, van der Waals, and hydrogen bond interactions are then defined in terms of these  $\sigma$ -profiles. One can use this formalism to compute the partition function, the Gibbs free energy, and many other important thermodynamic quantities, including the pseudo-chemical potential ( $\mu^*$ ) (i.e., the Gibb's free energy per molecule without the mixing entropy contribution). If the pseudo-chemical potential of a solute molecule in a solution containing  $x$  mole-fraction of the solute is  $\mu_{\text{solution}}^*(x, T)$ , and that in the solute's own liquid environment is  $\mu_{\text{self}}^*(T)$ , then under dilute conditions, the solubility (in mole-fraction) is given by the expression [22]:

$$x = \exp[\{\mu_{\text{self}}^*(T) - \mu_{\text{solution}}^*(x, T)\} / k_B T] \quad , \quad (1)$$

where  $T$  is the absolute temperature and  $k_B$  the Boltzmann constant, respectively.

The COSMO-RS program was originally developed with the aim of modeling condensed phases, primarily liquid, with solubility and liquid-liquid phase equilibrium (LLE) being one of its primary application domains. For a solid dissolving into a liquid solvent one needs to include an additional contribution due to the heat of fusion. From

extensive tests on the aqueous solubility of a large dataset of drug molecules and organic solutes it appears that COSMO-RS incurs an average error of the order of 0.3-0.5 log units [23]. Based on this, an accuracy of the computed solubility to within a factor of 2–3 can be considered reasonable. At the same time the COSMO-RS errors are not random, but are rather systematic within classes of solvents. Therefore, one can still expect to obtain useful trends from such calculations.

One challenge for the present application is that the solute species ( $\text{CO}_2$ ) is dissolving not from the solid or liquid, but from the gas phase. Although, there is a standard prescription of computing gas solubility with COSMO-RS that involves the experimental vapor pressure, this can lead to a severe overestimation of  $\text{CO}_2$  solubility at a given pressure and temperature as compared to experimental results [24]. As an alternative strategy, we have recently shown that the following equation works better with consistent accuracy [25]:

$$P = \frac{P^0}{\phi(P, T)} x \exp[\{\mu_{\text{solution}}^*(x, T) - \mu_{\text{ig}}^*(T)\} / k_B T], \quad (2)$$

where  $x$  is the mole-fraction gas-solubility at pressure  $P$  and temperature  $T$ ,  $\phi(P, T)$  is the fugacity coefficient of the dissolving gas, and  $\mu_{\text{ig}}^*$  the dilute-limit pseudo-chemical potential of the ideal dissolving gas defined at a low reference pressure of  $P^0 = 1$  bar. To use eq. (2) successfully we adopt the following strategy:

- The chemical potentials  $\mu_{\text{solution}}^*(x, T)$  are computed by COSMO-RS using the commercial code COSMOtherm version C2.1, Release 01.10 [26]. For this, the  $\sigma$ -profiles are first obtained by self-consistently computing the electronic charge density of each molecule, both the solute ( $\text{CO}_2$ ) and the solvent (a series of IL's). Our calculations employ the Density-Functional-Theory (DFT) code Turbomole [27, 28], the BP exchange-correlation functional [29, 30], and an all-electron representation in the triple-zeta valence basis set with polarization (TZVP) [31, 32]. For each IL a separate  $\sigma$ -profile is constructed for the cation and the anion, and the solvent represented as a 50:50 molar mixture of the two fragments [22].
- The fugacity coefficient  $\phi$  is computed by the standard formula:

$$\ln(\phi) = (k_B T)^{-1} \int_0^P (V - k_B T / P) dP$$

To evaluate the above integral we use the Soave-Redlich-Kwong (SRK) [33, 34] equation of state (EOS) for  $\text{CO}_2$ . Fig. 1 displays results for the fugacity coefficient of  $\text{CO}_2$  as a function of  $P$  for three different temperatures of our interest, where we have used  $\text{CO}_2$  SRK parameters. As expected,  $\phi$  monotonically decreases as a function of

increasing  $P$  and decreasing  $T$ . At  $T$  around  $T_c$ , the SRK EOS is known to become less accurate for  $P$  greater than  $P_c$  [33]. Thus, our analysis was confined to  $P$  not much higher than  $P_c = 73.7$  bar (for  $\text{CO}_2$ ).

- Finally, a proper computation of  $\mu_{ig}^*(T)$  within the COSMO-RS framework would involve a complete analysis of the differences between partition function of a free molecule and a molecule in the condensed phase, including rotational, translational, vibrational, and zero-point contributions. Fortunately, in practice, a simple empirical free-energy correction term appears sufficient for the subcritical region  $T < 0.7 T_c$  [22]. However, for the near-critical and supercritical region of our interest, corrections to the COSMOtherm-computed  $\mu_{ig}^*$  became necessary. From extensive numerical experiments, we found that the following simple 2-parameter formula works well in the 20-100 °C temperature range:

$$\mu_{ig}^*(T) = \mu_{ig}^*(T_c) + \alpha(T - T_c). \quad (3)$$

## Results

In our previous work [25] we tested the above formalism on a limited dataset and recommended values of  $\mu_{ig}^*(T_c) = -4.43$  kcal/mol and  $\alpha = -0.02$  kcal/mol/K. The emphasis in that work was placed on establishing the validity of the above computational scheme and looking for consistency in solubility trends rather than the optimization of the accuracy of the predicted solubility. When a larger dataset of  $\text{CO}_2$  solubility measurements is included, the computed solubility using the above parameter values displays a significant deviation from the 45° line (see Fig. 2 (left)), although there is still a strong linear correlation. In other words, the original parameter values of  $\mu_{ig}^*(T_c)$  and  $\alpha$  introduces a bias, as recently pointed out by ref. [35]. As a remedy, these authors introduce an additional pressure-dependent parameter.

In this work we show that it is unnecessary to introduce any additional parameters, either involving pressure-dependence or non-linear dependence on temperature. Rather, a simple optimization of the parameter values to  $\mu_{ig}^*(T_c) = -4.10$  kcal/mol and  $\alpha = -0.019$  kcal/mol/K solves the problem, as shown in Fig. 2 (right). Note that the experimental data points correspond to several temperatures varying between 20 °C and 100 °C, and the accuracy of the results do not deteriorate at elevated temperatures. The mean deviation in predicted fugacity as compared to the experimental values (for a given solubility level of  $\text{CO}_2$ ) is  $\sim 5.5$  bar. Above pressures of 15 bar the average accuracy of prediction is within 20%. At low pressures (a few bars or less) the predicted solubility displays Henry's behavior. However, from a few limited calculations we found that the predicted Henry's constant could show significant deviation from experimental values, up to 50% or larger.

Using the new optimized parameters we screened for the IL solvents with the best solubility of  $\text{CO}_2$  in the range of pressures 30-50 bar and at  $T = 40$  °C. Fig. 3 displays the computed results at  $P = 50$  bar as a function of twelve different cations for a fixed anion  $[\text{Tf}_2\text{N}]$ , one of the most commonly studied anions with a high mole-fraction

solubility for CO<sub>2</sub>. Fig. 3 plots the CO<sub>2</sub> solubility both in mole-fraction ( $x$ ) and in a more practical molality scale, defined by the number of moles of CO<sub>2</sub> dissolved per kg of the solvent:

$$\text{molality (mol/kg)} = \frac{x}{(1-x)M_w},$$

where  $M_w$  is the molecular weight of a solvent ion-pair in kg/mol. The molality scale emphasizes the amount (i.e. mass) of solvent required to dissolve a given amount of CO<sub>2</sub>.

The results in Fig. 3 are arranged from left to right in the increasing order of the molality values. The most notable results can be summarized as: (1) the mole-fraction solubility increases as a function of the size of the functional group on the cations, as evident from the orderings: [emim] < [bmim] < [hmim] < [omim]; [tbp] < [ttp]; [tma] < [tea] < [tba]; and [hmg] < [ppg]; (2) for the ions chosen in this group, the molal solubility follows the same order as the mole-fraction solubility in spite of the increasing molecular weight of the larger functional groups. The only exception is [ttp] < [tbp], and is clearly a result of [ttp] possessing a much higher molecular weight than [tbp] (see Table 1). The case of [ttp] having lower molal solubility of CO<sub>2</sub> than [tbp] implies that the molal solubility within a cationic class attains a maximum value for ions of masses somewhere in the range 200-400 g/mol depending on the class; (3) by comparing different classes with similar functional groups we can draw the conclusion that the molal solubility increases in the order imidazolium < phosphonium ~ ammonium < guanidinium.

To test the last point, and to see which cation-anion combination (within our limited set) could lead to an IL with the maximum molal solubility of CO<sub>2</sub>, we computed the CO<sub>2</sub> solubility in six different anions ([BF<sub>4</sub>], [PF<sub>6</sub>], [Tf<sub>2</sub>N], [NO<sub>3</sub>], [TfO], and [FEP]) and three different cations ([omim], [tba], and [ppg]). The three cations chosen are the most efficient (within our data set) solvent representatives of the three classes imidazolium, ammonium, and guanidinium respectively (the results for phosphonium are very similar to ammonium and are not reported separately). Fig. 4 displays the results at  $T = 40$  °C and  $P = 30$  bar. The most notable results are: (1) for the imidazolium class [FEP] leads to the highest mole-fraction solubility, in agreement with a previous publication [36] while Tf<sub>2</sub>N is a close second. However, within the ammonium and the guanidinium classes, [FEP] is not as efficient. [Tf<sub>2</sub>N] appears to possess the highest or near-highest mole-fraction across all cationic classes, which perhaps justifies the reason for it being one of the most studied IL anions; (2) for both ammonium and guanidinium classes the molal solubility increases in the order [FEP] < [Tf<sub>2</sub>N] < [PF<sub>6</sub>] < [TfO] < [BF<sub>4</sub>] < [NO<sub>3</sub>]. This order nearly holds for the Imidazolium class as well, with the molal solubility of the middle four groups being close to each other. In particular, note that [FEP] is the least efficient and [NO<sub>3</sub>] the most efficient for all cations in terms of molal solubility; (3) overall, the efficiency order in terms of molal solubility appears to be imidazolium < ammonium < guanidinium, as also seen in Fig. 3. In particular, [PPG][NO<sub>3</sub>] possess the highest molal solubility of CO<sub>2</sub>, roughly 2.6 times (i.e. 160 % higher) as compared to [omim][NO<sub>3</sub>], the highest value for the most commonly studied imidazolium class. Interestingly, for the imidazolium class the [NO<sub>3</sub>] group does not stand out in its mole-fraction solubility of CO<sub>2</sub>. That could be the reason why much attention was not paid to it in our previous study [25], and [PPG][BF<sub>4</sub>] was assigned the most efficient solvent within the data set. One should note that the molal solubility in

[omim][NO<sub>3</sub>] is high within the imidazolium class simply because of the small size of the [NO<sub>3</sub>] anion. However, for the ammonium and guanidinium groups even the mole-fraction solubility is the highest or near-highest in presence of the [NO<sub>3</sub>] anion. This, in combination with the small size of [NO<sub>3</sub>] makes the molal solubility of CO<sub>2</sub> in [NO<sub>3</sub>] much higher than other anions. This is especially true for [PPG], where the mass of the cation is also smaller compared to [omim] or [TBA].

### Conclusions

In summary, we show that the two-parameter model previously introduced [25] is adequate for accurate prediction of CO<sub>2</sub> solubility in diverse ionic liquids over a range of temperatures and pressures. The previous parameters were not properly optimized and led to a bias that has been corrected in the present work. With these new parameters, the average accuracy of prediction is within 20% in pressures > 15 bar. The Henry's constant prediction (low pressures) is more in error, with an average error of ~ 50%, which is still in line with factors of 2-3 inaccuracy inherent in COSMO-RS when tested against the aqueous solubility of drug molecules [23]. With these new parameters we show that the [NO<sub>3</sub>] anion is particularly efficient in dissolving CO<sub>2</sub>, and in combination with ammonium or guanidinium cations should lead to much higher molal solubility as compared to the highest experimentally observed value within the imidazolium class. Although the method presented here is simple, one needs to exert caution in applying to a new IL system because of inherent inaccuracies of COSMO-RS in dealing with certain functional groups [22].

Finally, we should point out that the method and analysis shown here is only one part of the puzzle that needs to be solved in order to make ILs a commercial success in carbon capture. There are several other considerations that need to be kept in mind, including: (1) the thermophysical properties of the IL, e.g., melting point, viscosity, and specific heat; (2) selectivity of CO<sub>2</sub> against other gases (e.g., N<sub>2</sub>, O<sub>2</sub>, S-containing pollutants, etc.); and (3) cost of IL synthesis. Also, physical dissolution is probably practical only when the CO<sub>2</sub> concentration in the feed stream is high. For post-combustion capture one may need task-specific ILs functionalized with amines [37, 38], so that a dilute amount of CO<sub>2</sub> can be captured through chemisorption.

**Acknowledgements:** This work was performed under the auspices of the U.S. Department of Energy by Lawrence Livermore National Laboratory under Contract DE-AC52-07NA27344.

References:

1. See: [http://en.wikipedia.org/wiki/Carbon\\_capture\\_and\\_storage](http://en.wikipedia.org/wiki/Carbon_capture_and_storage).
2. Rochelle, G. T. *Science* **2009**, *325*, 1652.
3. Welton, T. *Chem. Rev.* **1999**, *99*, 2071; Holbrey, J. D.; Seddon, K. R. *Clean Products and Processes* **1999**, *1*, 223; Dupont, J.; de Souza, R. F.; Suarez, P. A. *Chem. Rev.* **2002**, *102*, 3667.
4. *Green Industrial Applications of Ionic Liquids* (Eds.: R. D. Rogers, K. R. Seddon, S. Volkov), NATO Science Series, Kluwer, Dordrecht, **2002**.
5. Ilconich, J. ; Myers, C.; Pennline, H.; Luebke, D. *J. Membrane Sci.* **2007**, *298*, 41.
6. Blanchard, L. A.; Hancu, D.; Beckman, E. J.; Brennecke, J. F. *Nature* **1999**, *399*, 28; Blanchard, L. A.; Brennecke, J. F. *Ind. Eng. Chem. Res.* **2001**, *40*, 2550.
7. Blanchard, L. A.; Gu, Z. Y.; Brennecke, J. F. *J. Phys. Chem. B* **2001**, *105*, 2437.
8. Aki, S. N. V. K.; Mellein, B. R.; Saurer, E. M.; Brennecke, J. F. *J. Phys. Chem. B* **2004**, *108*, 20355.
9. Zhang, S. J.; Yuan, X. L.; Chen, Y. H.; Zhang, X. P. *J. Chem. Eng. Data* **2005**, *50*, 230.
10. Muldoon, M. J.; Aki, S. N. V. K.; Anderson, J. L.; Dixon, J. K.; Brennecke, J. F. *J. Phys. Chem. B* **2007**, *111*, 9001.
11. Schilderman, M.; Raeissi, S.; Peters, C. J. *Fluid Phase Equilibria* **2007**, *260*, 19.
12. Kumelan, J.; Kamps, A. P-S.; Tuma, D.; Maurer, G. *J. Chem. Eng. Data* **2006**, *51*, 1802.
13. Kumelan, J.; Kamps, A. P-S.; Tuma, D.; Maurer, G. *J. Chem. Thermodynamics* **2006**, *38*, 1396.
14. Cadena, C.; Anthony, J. L.; Shah, J. K.; Morrow, T. I.; Brennecke, J. F.; Maginn, E. J. *J. Am. Chem. Soc.* **2004**, *126*, 5300.
15. Deschamps, J.; Gomes, M. F. C.; Padua, A. A. H. *ChemPhysChem* **2004**, *5*, 1049.
16. Bhargava, B. L.; Balasubramanian, S. *Chem. Phys. Lett.* **2007**, *444*, 242.
17. Torrie G.M.; Valleau, J.P. *J. Comput. Phys.*, 1977, **23**, 187.
18. Jorgensen, W.L.; Buckner, J.K.; Boudon, S.; Tirado-Reeves, J. *J. Chem. Phys.*, 1988, **89**, 3742.

19. Mezei, M.; Beveridge, D. L. *Ann. NY Acad. Sci.*, 1986, **482**, 1.
20. Ciccotti, G.; Ferrario, M.; Hynes, J.T.; Kapral, R. *Chem. Phys.*, 1989, **129**, 241.
21. Klamt, A.; Schüürmann, G. *J. Chem. Soc. Perkin. Trans.* **1993**, *2*, 799.
22. Klamt, A. *COSMO-RS: From Quantum Chemistry to Fluid Phase Thermodynamics and Drug Design*, Elsevier, 2005.
23. Klamt, A.; Eckert, F.; Hornig, M.; Beck, M. E.; Burger, T. *J. Comp. Chem.* **2001**, *23*, 275.
24. Kolář, P. *et al.*, *Fluid Phase Equilibria* **2005**, *228*, 59.
25. Maiti, A. *ChemSusChem* **2009**, *2*, 628.
26. Available from Cosmologic Inc., <http://www.cosmologic.de>.
27. Ahlrichs, R.; Bär, M.; Häser, M.; Horn, H.; Kölmel, C. *Chem. Phys. Lett.* 1989, **162**, 165.
28. Schäfer, A.; Klamt, A.; Sattel, D.; Lohrenz, J. C. W.; Eckert, F. *Phys. Chem. Chem. Phys.* 2000, **2**, 2187.
29. Becke, A. D. *Phys. Rev. A* 1988, **38**, 3098.
30. Perdew, J. P. *Phys. Rev. B* 1986, **33**, 8822; Perdew, J. P. *Phys. Rev. B* 1986, **34**, 7406.
31. Eichkorn, K.; Weigend, F.; Treutler, O.; Ahlrichs, R. *Theor. Chim. Acta* 1997, **97**, 119.
32. Schäfer, A.; Huber, C.; Ahlrichs, R. *J. Chem. Phys.* 1994, **100**, 5829.
33. Soave, G. *Chem. Eng. Sci.* **1972**, *27*, 1197.
34. Tassios, D. P. *Applied Chemical Engineering Thermodynamics*, Springer-Verlag, Berlin, Germany (1993).
35. Mortazavi-Manesh, S.; Satyro, M.; Marriott, R. A. *Can. J. Chem. Eng.* **2012**, DOI 10.1002/cjce.21687.
36. Zhang, X.; Liu, Z.; Wang, W. *AIChE J.* **2008**, *54*, 2717.
37. Bates, E. D.; Mayton, R. D.; Ntai, I.; Davis, J. H., *J. Am. Chem. Soc.* **2002**, *124*, 926.
38. Gurkan, B. E. *et al.*, *J. Am. Chem. Soc.* **2010**, *132*, 2116.

Table 1. Chemical names, molecular weight, and class categories of the cations in Fig. 3.

Acronym	Chemical Name	Molecular Weight (g/mol)	Class
[emim]	1-ethyl-3-methyl-imidazolium	111.2	imidazolium
[bmim]	1-butyl-3-methyl-imidazolium	139.2	imidazolium
[hmim]	1-hexyl-3-methyl-imidazolium	167.3	imidazolium
[omim]	1-octyl-3-methyl-imidazolium	195.3	imidazolium
[tma]	tetra-methyl-ammonium	74.1	ammonium
[tea]	tetra-ethyl-ammonium	130.3	ammonium
[tba]	tetra-n-butyl-ammonium	242.5	ammonium
[tbp]	tetra-butyl-phosphonium	259.4	phosphonium
[ttp]	trihexyl-tetradecyl-phosphonium	483.9	phosphonium
[tmg]	tetra-methyl-guanidinium	116.2	guanidinium
[hmg]	hexa-methyl-guanidinium	144.2	guanidinium
[ppg]	n, n, n, n, n-pentamethyl-n-propyl-guanidinium	172.3	guanidinium

Table 2. Chemical names, molecular weight, and class categories of the anions in Fig. 4.

Acronym	Chemical Name	Molecular Weight (g/mol)
[BF <sub>4</sub> ]	tetrafluoroborate	86.8
[PF <sub>6</sub> ]	hexafluorophosphate	145.0
[Tf <sub>2</sub> N]	bis(trifluoromethylsulfonyl)imide	280.1
[NO <sub>3</sub> ]	nitrate	62.0
[TfO]	trifluoromethanesulfonate	149.1
[FEP]	tris(pentafluoroethyl)trifluorophosphate	445.0

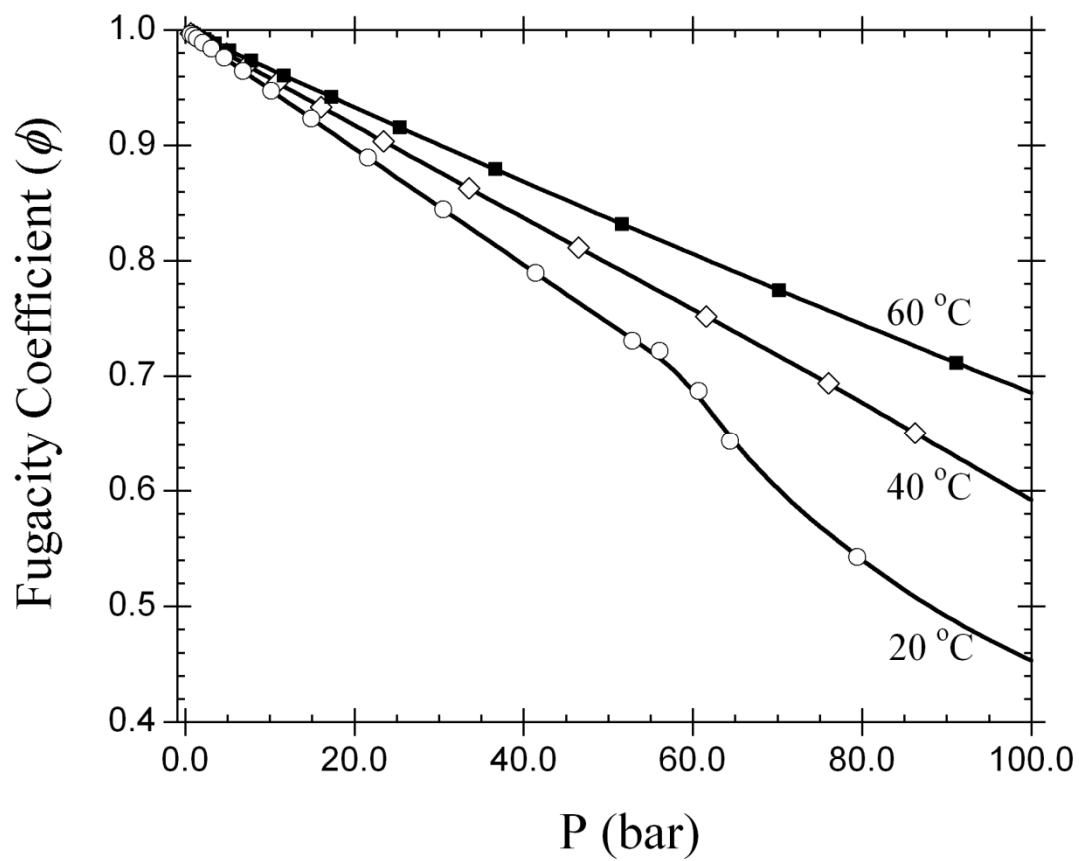


Fig. 1. Fugacity coefficient ( $\phi$ ) of CO<sub>2</sub> at three different temperatures computed using the SRK equation of state.

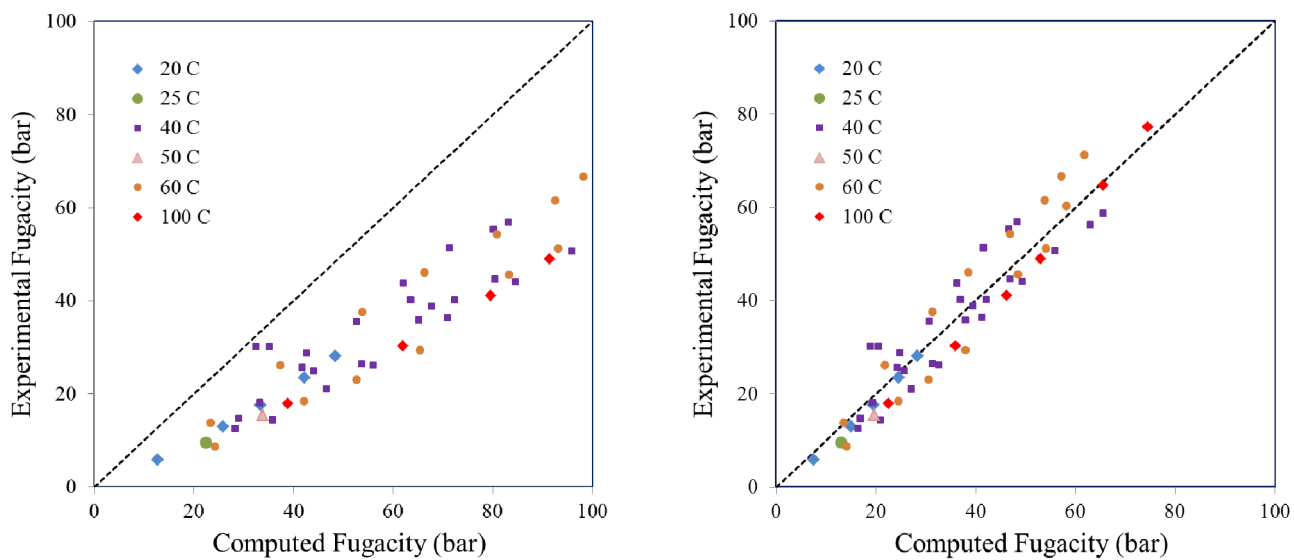


Fig. 2. Computed versus experimental fugacity using the two-parameter model for  $\mu_{ig}^*(T)$  (see eq. (3) of text): (left) using previous parameters from ref. [25], (right) presently optimized parameters with values  $\mu_{ig}^*(T_c) = -4.10$  kcal/mol and  $\alpha = -0.019$  kcal/mol/K. The experimental data are from references [6-13], and correspond to different temperatures varying between 20–100 °C (color coded).

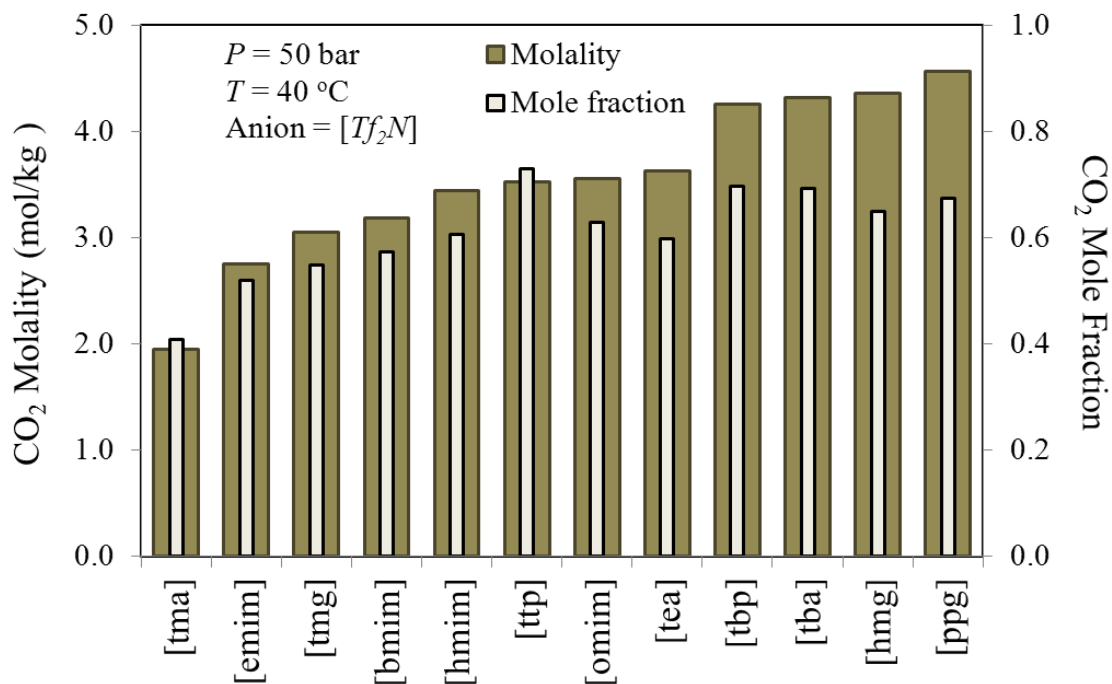


Fig. 3. Computed CO<sub>2</sub> solubility in various ILs as a function of cations for a fixed anion  $[\text{Tf}_2\text{N}]$  at  $T = 40 \text{ }^\circ\text{C}$  and  $P = 50 \text{ bar}$ . The solubility is computed in two different scales: molality scale (mol CO<sub>2</sub>/ kg solvent) and mole-fraction. Fully functionalized ammonium, phosphonium, and guanidinium cations appear to possess higher CO<sub>2</sub> solubility as compared to imidazolium, the most commonly studied class of cations in the experimental literature. In this group, the IL  $[\text{ppg}][\text{Tf}_2\text{N}]$  possesses the highest molal solubility, while the IL  $[\text{ttp}][\text{Tf}_2\text{N}]$  possesses the highest mole-fraction solubility of CO<sub>2</sub>. The IL acronyms are explained Tables 1 and 2.

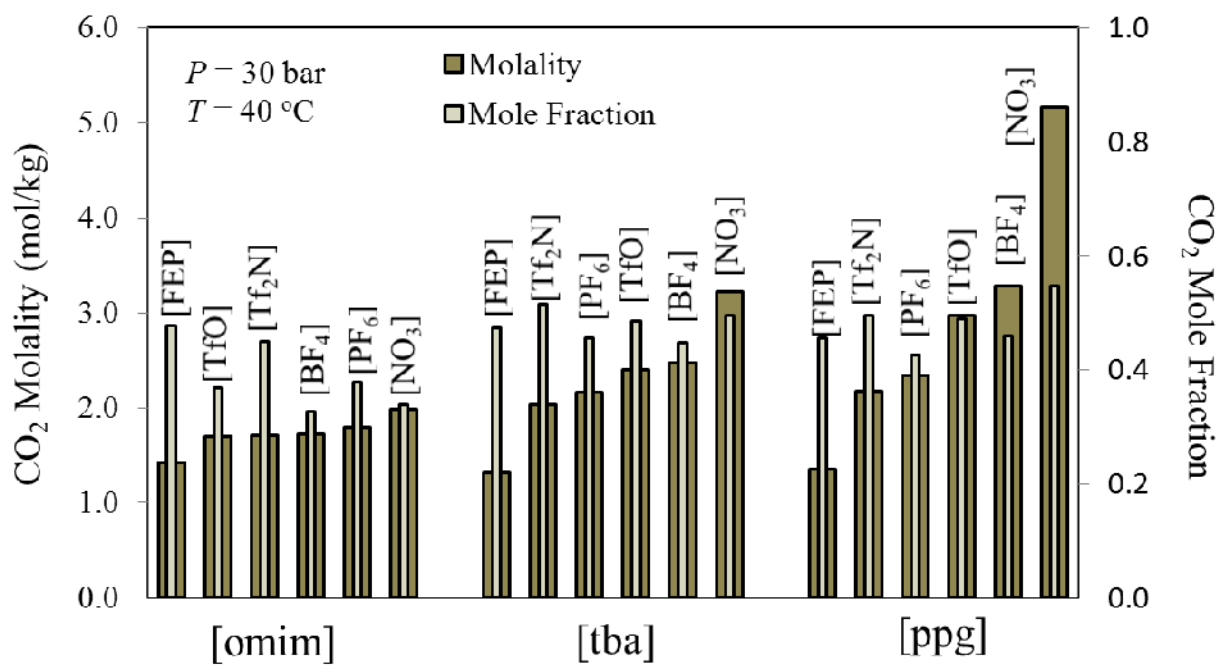


Fig. 4. Computed CO<sub>2</sub> solubility in various ILs as a function of six different anions and three different cations belonging to the imidazolium ([omim]), ammonium ([tba]), and guanidinium ([ppg]) classes; T = 40 °C and P = 30 bar. The solubility is computed in two different scales: molality scale (mol CO<sub>2</sub>/ kg solvent) and mole-fraction.